

Antineoplastic Agents. 509. Synthesis of Fluorcombstatin Phosphate and Related 3-Halostilbenes^{||,1}

George R. Pettit,^{*,†} Mathew D. Minardi,[†] Heidi J. Rosenberg,[†] Ernest Hamel,[‡] Michael C. Bibby,[§] Sandie W. Martin,[§] M. Katherine Jung,[⊥] Robin K. Pettit,[†] Timothy J. Cuthbertson,[†] and Jean-Charles Chapuis[†]

Cancer Research Institute and Department of Chemistry and Biochemistry, Arizona State University, P.O. Box 872404, Tempe, Arizona 85287-2404, Screening Technologies Branch, Developmental Therapeutics Program, Division of Cancer Treatment and Diagnosis, National Cancer Institute at Frederick, National Institutes of Health, Frederick, Maryland 21702, University of Bradford, Cancer Research Unit, West Yorkshire BD7 1DP, United Kingdom, and Science Applications International Corp., National Cancer Institute at Frederick, National Institutes of Health, Frederick, Maryland 21702

Received March 14, 2005

The present SAR study of combretastatin A-3 (**3a**) focused on replacement of the 3-hydroxyl group by a series of halogens. That approach with *Z*-stilbenes resulted in greatly enhanced (>10–100-fold) cancer cell growth inhibition against a panel of human cancer cell lines and the murine P388 lymphocytic leukemia cell line. Synthesis of the 3-fluoro-*Z*-stilbene designated fluorcombstatin (**11a**) and its potassium 3'-*O*-phosphate derivative (**16c**) by the route **7** → **8a** → **11a** → **14** → **16c** illustrates the general synthetic pathway. The 3'-*O*-phosphoric acid ester (**15**) of 3-bromo-*Z*-stilbene **13a** was also converted to representative cation salts to evaluate the potential for improved aqueous solubility, and the potassium salt (16 mg/mL in water) proved most useful. The fluoro (**11a**), chloro (**12a**), and bromo (**13a**) halocombstatins were nearly equivalent to combretastatin A-4 (**1a**) as inhibitors of tubulin polymerization and of the binding of colchicine to tubulin. The tubulin binding in cell-free systems was also retained in human umbilical vein endothelial cells. All three halocombstatins retained the powerful human cancer cell line inhibitory activity of combretastatin A-4 (**1a**) and proved superior to combretastatin A-3 (**3a**). In addition, the halocombstatins targeted Gram-positive bacteria and *Cryptococcus neoformans*.

The African Bush Willow *Combretum caffrum* (Combretaceae) has proved to be a very important source of new cancer cell growth inhibitory constituents that we discovered beginning in 1979 and named combretastatins.² The most potent cancer cell line inhibitor among a series of *cis*-stilbene constituents (Figure 1) was combretastatin A-4 (**1a**, CA4), and its sodium phosphate (CA4P) derivative (**1b**) was advanced to Phase I human cancer clinical trials in 1998.² Overall results continue to be promising, and human cancer Phase II and combination (Phase 1b) trials with CA4P (**1b**) are currently underway. Antivascular,³ antiangiogenesis,⁴ and general antimetastatic⁵ activities of CA4P, as well as its synergistic utility in combination^{5f} with other anticancer drugs, radioimmunotherapy,^{6a} and hyperthermia,^{6b} are all areas of active cancer research interest.

After the discovery of CA4, we⁷ and others⁸ have been conducting SAR investigations of this relatively simple but biologically fascinating molecule. In addition, we have been extending SAR insights derived from combretastatins A-1 (**2a**),^{9a,b} A-2,^{7a} and A-3 (**3a**)^{9c} to new antineoplastic agents. Now we report a series of structural modifications of combretastatin A-3 (**3a**) and its phosphate prodrug (**3b**) by replacing the 3-hydroxy group with halogens and with primary focus on the fluoro substituent. Since the phosphate ester derivative of combretastatins A-1–A-4 proved to be an effective method for increasing aqueous solubility

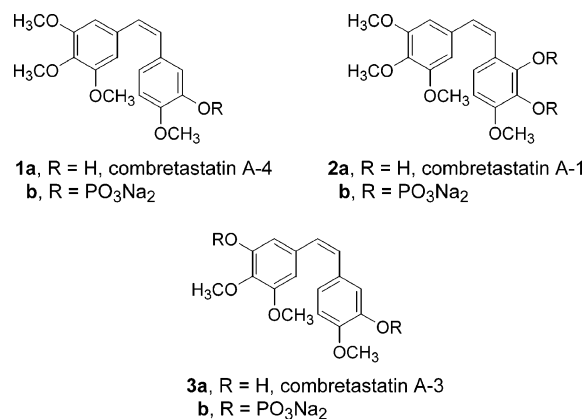


Figure 1.

and transport in vivo, we also synthesized phosphate ester derivatives of the 3-fluoro-¹⁰ and 3-bromostilbenes.¹¹

Results and Discussion

Preparation of the stilbenes was accomplished as shown in Scheme 1 and Figure 2. Phosphonium bromide **7** was prepared as previously described,^{9c} and condensation with the appropriate halobenzaldehyde^{10–12} using *n*-butyllithium in THF led to silyl-protected stilbenes **8**–**10**. Subsequent deprotection (Scheme 1) with tetrabutylammonium fluoride afforded 3-halostilbenes **11**–**13**. The *Z*-isomers **11a** and **13a** were phosphorylated⁹ using dibenzyl phosphite, diisopropylethylamine, *N,N*-(dimethylamino)pyridine, and carbon tetrachloride in acetonitrile to provide bisbenzyl phosphates **14** and **15**. Debenzylation of the phosphate esters (**14** and **15**) was achieved using trimethylsilylbromide^{9b,c} followed by the corresponding base to produce phosphates **16** and **17**. Compounds **18** and **19** were used to synthesize

^{||} Dedicated to the memory of Professor Thomas A. Connors (1934–Feb 4, 2002), a remarkably effective advocate of new anticancer drug discovery and development. Please refer to Newell et al. (*Br. J. Cancer* **2003**, *89*, 437–454).

^{*} To whom correspondence should be addressed. Tel: 480-965-3351. Fax: 480-965-8558.

[†] Arizona State University.

[‡] STB, NCI, Frederick.

[§] University of Bradford.

[⊥] SAIC, NIH, Frederick.

Scheme 1

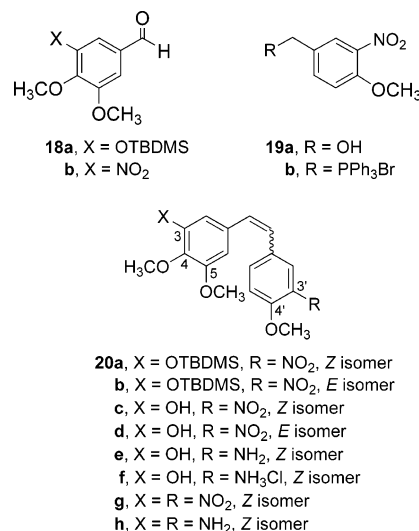
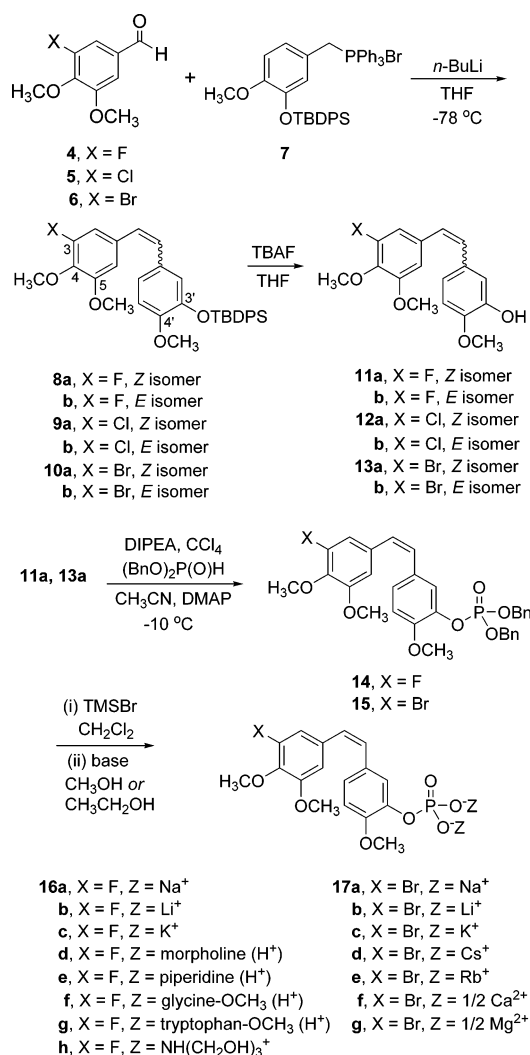


Figure 2.

equimolar to the tubulin concentration, binding of the radiolabeled ligand was inhibited by 75–89%. Interestingly, the lowest and highest inhibitory effects were observed with stilbenes **11a** and **13a**, the two compounds that displayed the greatest inhibitory effects in the polymerization assay.

In an earlier study,¹³ combretastatin A-3 (**3a**, with a C-3 hydroxyl instead of a methoxyl or halogen) was found to be about half as active as combretastatin A-4 (**1a**) as an inhibitor of tubulin assembly, about one-fifth as active as an inhibitor of colchicine binding to tubulin, and about one-seventh as active as an inhibitor of cancer cell growth. A related finding was that elimination of the C-3 substituent entirely, by replacing it with a hydrogen atom, resulted in about a 7-fold reduction in inhibitory effect on polymerization and complete loss of cytotoxic activity.¹⁴ Thus, the optimal activity observed with combretastatin A-4 (**1a**) and the three halocombstatins suggests a C-3 substituent of some size is necessary where the fluorine atom may represent a minimum and a C-3 methoxy group is quite favorable. Therefore, it seems unlikely that the predominant effect of the substituent results from direct enhancement of the interaction of ligand with protein. The A-ring substituents most likely cause the active *cis*-stilbenes to assume with greater probability a conformation that favors the drug–tubulin interaction.

The concept of antiangiogenesis as a therapeutic approach is now robustly pursued as a promising novel antitumor strategy.¹⁵ Previous investigations have also shown that combretastatin A-4 disrupts the microtubules of human umbilical vein endothelial cells (HUVECs) in culture.^{16a} These studies confirmed that the tubulin-binding properties shown in cell-free systems are retained when the compound enters cells and that tubulin binding is a significant component of the biological activity. In the present study, the ability of stilbenes **11a** and **12a** to disrupt microtubules in HUVECs was determined. HUVECs were isolated according to the method of Jaffe et al.^{16b} Loss of cellular microtubules and disruption of cell division (binucleated cells) were clearly seen following treatment of HUVECs with halocombstatins **11a** and **12a** for 30 min at a concentration of $1\text{ }\mu\text{M}$ (see Figure 4). Stilbenes **11a** and **12a** caused marked cell rounding and depolymerization of tubulin under similar conditions (scoring = ++ at 30 min), but stilbene **12a** appeared slightly more potent (Table 3). The tubulin in HUVECs exposed to $1\text{ }\mu\text{M}$ **12a** for $\geq 1\text{ h}$ appeared mainly depolymerized with only a few microtu-

the nitro- and aminostilbenes **20a–h**, for purposes of comparison (Figure 2).

Compared to the related combretastatins, the new *Z*-halostilbenes all showed very strong inhibition of cancer cell growth (Table 1). Their cancer cell growth inhibitory properties were stronger than those of combretastatin A-3 (**3a**) and equivalent to combretastatin A-4 (**1a**). The nitro- and aminostilbenes (**20c–h**) proved to be generally less active. The strong inhibitory activities of stilbenes **11a** and **13a** were retained upon conversion to phosphate salts and displayed markedly better aqueous solubility than their phenol precursors. As expected,⁹ all of the *E* geometrical isomers evaluated proved to be much less effective as inhibitors of cancer cell growth.

Because of their potent cancer cell line inhibitory activity, the three halocombstatins (**11a**, **12a**, and **13a**) were compared to combretastatin A-4 (**1a**) with respect to inhibitory effects on tubulin polymerization and on the binding of [^3H]colchicine to tubulin (Table 2). These experiments demonstrated that all were essentially identical in their apparent interactions with tubulin. The three halocombstatins inhibited the polymerization reaction with IC_{50} values of $1.5\text{--}1.6\text{ }\mu\text{M}$, versus an IC_{50} value of $1.8\text{ }\mu\text{M}$ for combretastatin A-4 (**1a**). The minor differences were within experimental error, as indicated by the standard deviations. Similarly, all three *cis*-stilbenes were highly potent inhibitors of the colchicine binding assay. When present at a concentration one-fifth that of [^3H]colchicine but

Table 1. Human Cancer Cell Line Growth Inhibition (GI₅₀ μg/mL) and Murine P388 Lymphocytic Leukemia Inhibitory Activity (ED₅₀ μg/mL) of Combretastatin A-1 (**2a**), A-3 (**3a**), A-4 (**1a**), Fluorcombstatin (**11a**), and Synthetic Modifications Including Phosphate Salts

compound	leukemia P388	pancreas BXPC-3	breast MCF-7	CNS SF268	lung-NSC NCI-H460	colon KM20L2	prostate DU-145
1a	0.0003	0.39		<0.001	0.0006	0.061	0.0008
1b	0.0004			0.036	0.029	0.034	
2a	0.251	4.4			0.74	0.061	0.17
2b	<0.01	1.5	0.024	0.036	0.038	0.53	0.034
3a	0.26	2.3	0.49	0.0083	0.19	1.2	0.0043
3b	0.305	2.8	0.92	0.052	0.45	3.5	0.048
11a	<0.0020	0.745	<0.0027	<0.0016	<0.0032	>1	0.0019
11b	0.253	2.2	0.051	0.35	0.18	0.53	0.18
12a	0.0024	0.32	0.0026	<0.00090	0.00026	0.27	0.00025
12b	0.027	0.59	0.041	0.048	0.034	1.4	0.038
13a	0.0021	0.64	0.00046	0.00050	0.00038	0.59	0.00082
13b	0.0174	1.6	0.14	0.18	0.15	1.2	0.13
16a	0.0298	0.59	0.0044	0.0051	0.0094	1.5	0.0036
16b	0.019	0.490	0.0038	0.040	0.0039	>1	0.0043
16c	0.0074	0.548	0.0040	0.0039	0.0043	>1	0.0037
16d	0.015	0.73	0.0079	0.0087	0.0050	>1	0.0046
16e	0.0040	0.39	0.011	0.0075	0.022	>1	0.011
16f	0.030	>1	0.0060	0.0073	0.0034	>1	0.0037
16g	0.014	0.033	0.0020	0.0027	0.0032	0.062	0.0018
16h	0.015	0.99	0.031	0.017	0.034	>1	0.019
17a	<0.01	0.093	0.0041	0.0034	0.0028	0.23	0.0046
17b	<0.01	0.13	0.0039	0.0030	0.0026	0.11	0.0066
17c	<0.01	0.20	0.0035	0.0032	0.0029	0.24	0.0028
17d	<0.01	0.15	0.0044	0.0064	0.0066	0.48	0.0079
17e	<0.01	0.56	0.043	0.023	0.041	2.6	0.042
17f	0.288	<0.001	0.0022	0.0022	0.0068	0.37	0.0063
1g	<0.01	0.074	0.0045	0.0053	0.0039	0.27	0.0045
17h	<0.01	0.17	0.0049	0.0067	0.0047	0.45	0.0049
17i	2.22	>10	3.2	4.1	2.9	>10	2.8
20c	0.402	2.5	0.49	0.62	0.31	1.8	0.39
20d	0.224	1.1	0.56	0.41	0.25	1.2	0.36
20e	0.0174	0.37	0.060	0.040	0.030	0.39	0.035
20f	0.0289	1.0	<0.010	0.0022	0.035	1.3	0.012
20g	>10	0.39	0.37	0.59	0.24	0.27	0.34
20h	0.0360	0.053	<0.010	0.076	0.014	0.030	0.044

Table 2. Inhibition of Tubulin Polymerization and Binding of [³H]Colchicine to Tubulin by Halocombstatins

compound	inhibition of polymerization IC ₅₀ (μM) ± SD	inhibition of colchicine binding % inhibition ± SD
1a	1.8 ± 0.2	81 ± 3
11a	1.5 ± 0.2	75 ± 6
12a	1.6 ± 0.2	85 ± 4
13a	1.5 ± 0.2	89 ± 2

bules apparent (scoring = +++, Table 3). In another series of experiments, fluorcombstatin (**11a**) was further evaluated against HUVECs in vitro. These cells showed significant sensitivity to the fluorcombstatin (**11a**): ED₅₀ 0.00025 μg/mL. Cord lengths as well as junction numbers were markedly reduced at both 0.01 and 0.001 μg/mL (Figure 3B and 3C) compared to untreated controls (Figure 3A). Such activity against endothelial cells is of the utmost interest, as these cells play a central role in the angiogenic process.

We previously reported that combretastatin A-3, but not its sodium phosphate prodrug, inhibited growth of the pathogenic fungus *Cryptococcus neoformans*.^{9c} In the present study, the halocombstatins were also subjected to antimicrobial evaluation. Susceptibility testing was performed by the reference broth microdilution assay.^{17,18} The antimicrobial activities of the halocombstatins were very similar, targeting Gram-positive bacteria and *C. neoformans* (Table 4). As with the sodium combretastatin A-3 prodrug,^{9c} the sodium phosphate derivative (**16a**) of fluorcombstatin (**11a**) did not retain significant antimicrobial activity (Table 4).

Experimental Section

General Experimental Procedures. All solvents (ether refers to diethyl ether) were redistilled, and reagents were

from commercial sources (Acros Organics, Sigma-Aldrich Co., Alfa Aesar, City Chemicals, or Lancaster Synthesis, Inc.). Solvent extracts of aqueous solutions were dried over anhydrous MgSO₄. Gravity column chromatography was performed using silica gel from VWR Scientific (70–230 mesh) or from E. Merck (230–400). Analtech silica gel GHLF plates were employed for TLC.

Melting points were determined with an electrochemical digital melting point apparatus and are uncorrected. NMR spectra were recorded employing Varian Gemini 300 or Varian Unity 400 instruments. Chemical shifts are reported in ppm downfield from tetramethylsilane as an internal standard in CDCl₃ or where noted in D₂O. High-resolution mass spectra were obtained with a Kratos Ms-50 instrument (Midwest Center for Mass Spectroscopy, University of Nebraska–Lincoln) or with a JEOL LCMate instrument (ASU). Elemental analyses were determined by Galbraith Laboratories, Inc., Knoxville, TN.

Heteronuclear couplings were seen in both the ¹H NMR and ¹³C NMR in the compounds containing fluorine. In the ¹³C NMR, some couplings were easy to distinguish, while others were more difficult. When the couplings were difficult to distinguish, all signals are noted in the data.

General Procedure for Synthesis of Dimethoxyhalobenzaldehydes. 3-Fluoro-4,5-dimethoxybenzaldehyde (4). To a stirred solution prepared from 100 mL of DMF and 5-fluorovanillin (lit.¹⁰ 1.0 g, 5.88 mmol) was added portionwise over 15 min sodium hydride (60% in mineral oil, 282 mg, 7 mmol). After 15 min, iodomethane (1.5 mL, 24 mmol) was added, and stirring continued for 16 h at RT. The reaction was terminated by the addition of H₂O, the mixture was extracted with hexane (3 × 100 mL), and solvents were removed in vacuo. Purification by flash chromatography on a column of silica gel using hexane–ethyl acetate (4:1) as eluent afforded a colorless solid (1 g, 93%): mp 51–53 °C (lit.¹¹ mp 52–53 °C);

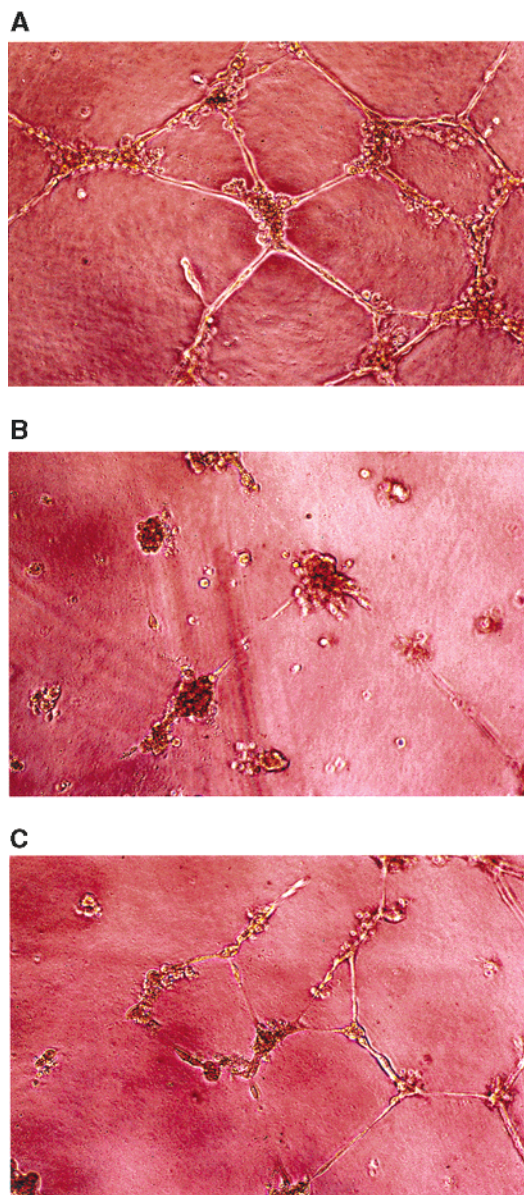


Figure 3. Morphological appearance of the cords in HUVEC cells. HUVEC were plated on Matrigel for 24 h. Control cells (A) differentiated into well-defined tube-like structures (note large amounts of cords and junctions). Cells that were exposed to **11a** (0.01 $\mu\text{g/mL}$) did not form complete tube-like structures (B) compared to the control (see marked reduction of cord lengths and junction numbers). Cells that were exposed to **11a** (0.001 $\mu\text{g/mL}$) formed a reduced number of such structures (C).

^1H NMR (300 MHz, CDCl_3) δ 3.94 (s, 3H), 4.05 (s, 3H), 7.24 (s, 1H), 7.26 (s, 1H), 9.82 (s, 1H).

3-Chloro-4,5-dimethoxybenzaldehyde (5). The preceding reaction was repeated with 5-chlorovanillin (10 g, 54 mmol) to give the title compound, which was isolated as recorded in the preceding experiment (**4**) to afford a colorless solid (10.4 g, 97%): mp 88–90 $^\circ\text{C}$ (lit.¹¹ mp 87–89 $^\circ\text{C}$); ^1H NMR (300 MHz, CDCl_3) δ 3.95 (s, 3H), 3.96 (s, 3H), 7.36 (d, 1H, $J = 1.5$ Hz), 7.50 (d, 1H, $J = 1.5$ Hz), 9.85 (s, 1H).

3-Bromo-4,5-dimethoxybenzaldehyde (6). The experiment was repeated with 5-bromovanillin (10 g, 43.3 mmol) as described for aldehyde **4**. Separation by flash chromatography on a column of silica gel using hexane–ethyl acetate (9:1) as eluent afforded a colorless solid (8 g, 75%): mp 64–65 $^\circ\text{C}$; ^1H NMR (300 MHz, CDCl_3) δ 3.94 (s, 3H), 3.95 (s, 3H), 7.39 (d, 1H, $J = 1.8$ Hz), 7.65 (d, 1H, $J = 1.8$ Hz), 9.85 (s, 1H).

General Procedure for the Stilbene Syntheses. 3-Fluoro-4,4',5-trimethoxy-3'-*O*-*tert*-butyldiphenylsilyl-*Z*-stilbene (**8a**). To a mixture of phosphonium salt **7^{9c}** (4.7 g, 6.5 mmol) and

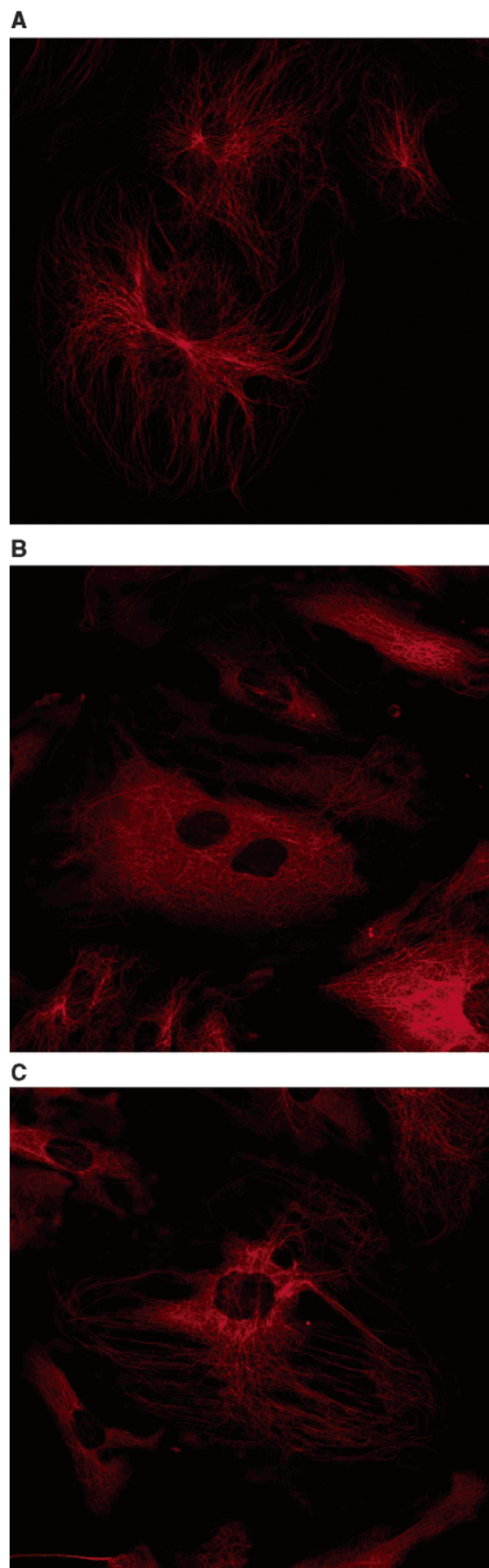


Figure 4. Morphological appearance of the microtubules in HUVECs: A, untreated control; B, after exposure to chlorocombstatin (**12a**, 1 μM for 30 min); C, after exposure to fluorcombstatin (**11a**, 1 μM for 30 min).

Table 3. Assessment of Microtubule Damage in Primary HUVECs Treated with **11a** or **12a** as Monolayer Cultures^a

stilbene	concentration				
	(μ M)	$t = 30$ min	$t = 1$ h	$t = 2$ h	$t = 4$ h
11a	0	normal	normal	normal	normal
	1	++	++	++	++
	10	+++	+++	+++	+++
12a	0	normal	normal	normal	normal
	1	++	++/+++	+++	+++
	10	+++	+++	+++	+++

^a Key for scoring of HUVECS: Normal: endothelial cells have normal microtubules. +: Slight depolymerization of tubulin visible; slight rounding of cells; many strands of microtubules still visible. ++: Marked cell rounding and microtubule disruption; depolymerization of microtubules apparent although some microtubules still visible. +++: Microtubules mainly depolymerized; occasional microtubules apparent; cells show marked rounding with transparent edges; rigid, fixed appearance.

tetrahydrofuran (25 mL, cooled to -78 °C) was added *n*-BuLi (2.6 mL, 2.5 M in hexane, 6.5 mmol, over 5 min). After 1 h, 3-fluoro-4,5-dimethoxybenzaldehyde (1 g, 5.4 mmol) in tetrahydrofuran (10 mL) was added over 30 min. The mixture was allowed to warm to RT and stirring continued for 16 h. The reaction was terminated by the addition of H₂O (50 mL), the product was extracted with ethyl acetate, solvents were removed in vacuo, and the residue obtained was subjected to flash column chromatography on silica gel using hexane–ethyl acetate (9:1) as eluent to afford *Z*-stilbene **8a** (1 g, 34%) as a clear oil: ¹H NMR (300 MHz, CDCl₃) δ 1.07 (s, 9H), 3.46 (s, 3H), 3.65 (s, 3H), 3.90 (d, 3H, $J_{\text{HF}} = 1.2$ Hz), 6.24 (d, 1H, $J = 12$ Hz), 6.33 (d, 1H, $J = 12$ Hz), 6.52–6.61 (m, 2H), 6.72–6.76 (m, 3H), 7.26–7.40 (m, 6H), 7.64–7.67 (m, 4H); ¹³C NMR (125 MHz, CDCl₃) δ 19.7, 26.6, 55.1, 56.0, 61.4 (d, $J_{\text{FC}} = 3.5$ Hz), 108.3, 108.3, 109.5 (d, $J_{\text{FC}} = 20$ Hz, *ortho* C), 111.7, 120.8, 122.4, 127.3, 127.4, 127.4, 127.7, 129.3, 129.5, 129.6, 130.3, 132.6 (d, $J_{\text{FC}} = 9$ Hz, *meta* C), 133.5, 134.7, 135.2, 135.8 (d, $J_{\text{FC}} = 14$ Hz, *ortho* C), 144.7, 149.8, 152.9, 152.9, 155.5 (d, $J_{\text{FC}} = 242$ Hz, *ipso* C); HRMS (calcd for C₃₃H₃₆FO₄Si [M + H]⁺ 543.2368, found 543.2372; *anal.* calcd for C₃₃H₃₅FO₄Si, C, H.

Further elution gave the *E*-isomer **8b** as a colorless solid, which was crystallized from hexane (1.2 g, 41%): ¹H NMR (300 MHz, CDCl₃) δ 1.14 (s, 9H), 3.56 (s, 3H), 3.91 (s, 3H), 3.93 (d, $J_{\text{HF}} = 1.2$ Hz), 6.45 (d, 1H, $J = 15.9$ Hz), 6.70–6.78 (m, 4H), 6.87 (d, 1H, $J = 2.1$ Hz), 6.93 (d, 1H, $J = 2.14$ Hz), 6.97 (d, 1H, $J = 2.1$ Hz), 7.34–7.45 (m, 6H), 7.73–7.77 (m, 4H); ¹³C NMR (75 MHz, CDCl₃) δ 19.7, 26.6, 55.2, 56.1, 61.3, 105.4, 106.4, 106.7, 112.6, 117.6, 120.6, 125.3, 127.5, 128.5, 129.6, 139.7, 133.1, 133.3, 133.6, 135.3, 145.1, 150.5, 153.5; HRMS calcd for C₃₃H₃₆FO₄Si 543.2368 [M + H]⁺, found 543.2392; *anal.* calcd for C₃₃H₃₅FO₄Si, C, H.

3-Chloro-4,4',5-trimethoxy-3'-O-tert-butylidiphenylsilyl-Z-stilbene (9a). The experimental procedure noted above (**8a**) was repeated with 3-chloro-4,5-dimethoxybenzaldehyde (2.8 g, 14 mmol) to yield the *Z*-isomer (1.6 g, 21%) as a clear oil: ¹H NMR (300 MHz, CDCl₃) δ 1.07 (s, 9H), 3.46 (s, 3H), 3.60 (s, 3H), 3.84 (s, 3H), 6.24 (d, 1H, $J = 12$ Hz), 6.34 (d, 1H, $J = 12$ Hz), 6.59 (d, 1H, $J = 7.5$ Hz), 6.66 (s, 1H), 6.73 (s, 1H), 6.73 (d, 1H, $J = 9$ Hz), 6.81 (s, 1H), 7.26–7.38 (m, 6H), 7.65 (dd, 4H, $J = 6.67$ Hz, $J = 1.2$ Hz); ¹³C NMR (125 MHz, CDCl₃) δ 19.8, 26.7, 55.1, 55.8, 60.7, 111.3, 111.7, 120.9, 122.4, 122.5, 127.1, 127.4, 127.8, 129.3, 129.5, 130.5, 133.6, 133.8, 135.3, 144.2, 144.7, 149.9, 153.1; HRMS calcd for C₃₃H₃₆ClO₄Si ³⁷Cl 561.2042 [M + H]⁺, found 561.2449, ³⁵Cl 559.2071 [M + H]⁺, found 559.1996; *anal.* calcd for C₃₃H₃₅ClO₄Si.

Continued elution of the chromatographic column led to the isolation of *E*-stilbene **9b** in 4.9 g, 62% yield as a clear oil: ¹H NMR (300 MHz, CDCl₃) δ 1.14 (s, 9H), 3.56 (s, 3H), 3.86 (s, 3H), 3.90 (s, 3H), 6.44 (d, 1H, $J = 16.5$ Hz), 6.74 (d, 1H, $J = 16.5$ Hz), 6.74 (s, 1H), 6.82 (d, 1H, $J = 1.5$ Hz), 6.87 (d, 1H, $J = 1.8$ Hz), 6.94 (dd, 1H, $J = 8.1$ Hz, $J = 2.1$ Hz), 6.99 (d, 1H, $J = 1.5$ Hz), 7.34–7.42 (m, 6H), 7.72–7.76 (m, 4H); ¹³C NMR (125 MHz, CDCl₃) δ 19.8, 26.7, 55.3, 55.1, 60.8, 108.4, 112.1, 117.7, 119.8, 120.6, 125.0, 127.5, 128.4, 128.8, 128.8, 129.6,

129.7, 133.6, 134.3, 135.4, 144.5, 145.2, 150.6, 153.7; *anal.* calcd for C₃₃H₃₅ClO₄Si.

3-Bromo-4,4',5-trimethoxy-3'-O-tert-butylidiphenylsilyl-Z-stilbene (10a). Employment of 3-bromo-4,5-dimethoxybenzaldehyde (8 g, 33 mmol) using the procedure for **8a** provided the *Z*-isomer (**10a**, 4.2 g, 21%) as a clear oil: IR 2962, 1730, 1510, 1267, 908, 735, 650 cm⁻¹; ¹H NMR (300 MHz, CDCl₃) δ 1.07 (s, 9H), 3.45 (s, 3H), 3.58 (s, 3H), 3.82 (s, 3H), 6.23 (d, 1H, $J = 12$ Hz), 6.32 (d, 1H, $J = 12$ Hz), 6.59 (d, 1H, $J = 8.1$ Hz), 6.69–6.75 (m, 1H), 6.97 (d, 1H, $J = 1.5$ Hz), 7.25–7.37 (m, 6H), 7.65 (dd, 4H, $J = 1.5$ Hz, $J = 8.1$ Hz); ¹³C NMR (100 MHz, CDCl₃) δ 19.8, 26.7, 55.1, 55.8, 60.6, 94.4, 111.7, 112.0, 117.2, 120.8, 122.4, 125.2, 126.9, 127.3, 129.2, 129.4, 130.4, 133.5, 134.4, 135.2, 144.7, 145.2, 149.8, 152.9; HRMS calcd for C₃₃H₃₅NaO₄SiBr ⁷⁹Br 625.1386 [M + Na]⁺, found 625.1364, ⁸¹Br 627.1365 [M + Na]⁺, found 627.1338.

Further elution of the chromatogram led to isolation of the *E*-isomer **10b** (8.1 g): IR 2934, 2859, 1710, 1510, 1275, 908, 732, 650 cm⁻¹; ¹H NMR (300 MHz, CDCl₃) δ 1.14 (s, 9H), 3.54 (s, 3H), 3.84 (s, 3H), 3.88 (s, 3H), 6.46 (d, 1H, $J = 12$ Hz), 6.71 (d, 1H, $J = 8.1$ Hz), 6.76 (d, 1H, $J = 12$ Hz), 6.85 (d, 1H, $J = 2.1$ Hz), 6.87 (d, 1H, $J = 2.1$ Hz), 6.94 (dd, 1H, $J = 8.4$ Hz, $J = 2.4$ Hz), 7.15 (d, 1H, $J = 2.4$ Hz) 7.30–7.44 (m, 6H), 7.74 (dd, 4H, $J = 1.8$ Hz, $J = 7.8$ Hz); ¹³C NMR (75 MHz, CDCl₃) δ 19.8, 26.6, 55.2, 56.0, 60.6, 109.2, 109.8, 112.1, 117.7, 120.6, 122.6, 124.8, 127.5, 128.8, 129.6, 133.6, 134.9, 135.3, 145.2, 150.6, 153.6.

3-O-tert-Butyldimethylsilyl-4,4',5-trimethoxy-3'-nitro-Z- and E-stilbenes (20a,b). The reaction was conducted in freshly distilled toluene (under argon) employing phosphonium bromide¹⁹ **19b** (41 g, 80.86 mmol, mp 109–111 °C, prepared in 95% yield, from benzyl alcohol¹⁹ **19a** and phosphorus tribromide in CH₂Cl₂), aldehyde **18a**^{9c} (11.3 g, 38.12), and sodium hydride (6.5 g, 162.5 mmol of 60% in mineral oil) at ice-bath temperature for 8 h followed by 14 h at ambient temperature. After initial isolation, the crude product was separated by flash column chromatography on silica gel (4:1 hexane–ethyl acetate) to provide *Z*-stilbene **20a** as a bright yellow oil (13.1 g, 55%): ¹H NMR (300 MHz) δ 0.08 (s, 6H), 0.94 (s, 9H), 3.70 (s, 3H), 3.77 (s, 3H), 3.92 (s, 3H), 6.34 (d, 0.5H, $J = 1.8$ Hz), 6.42 (d, 1H, $J = 12$ Hz), 6.43 (d, 0.5H, $J = 2.1$ Hz), 6.54 (d, 1H, $J = 12$ Hz), 6.93 (d, 0.5H, $J = 8.7$ Hz), 6.97 (d, 1H, $J = 8.7$ Hz), 7.33 (dd, 1H, $J = 1.8$ Hz, $J = 8.3$ Hz), 7.41 (dd, 0.5H, $J = 2.1$ Hz, $J = 8.9$ Hz), 7.65 (d, 0.5H, $J = 2.1$ Hz), 7.75 (d, 0.5H, $J = 2.1$ Hz); HRMS calcd for C₂₃H₃₂NO₆Si 446.1998 [M + H]⁺, found 446.2385.

Continued elution of the chromatographic column led to the isolation of *E*-stilbene **20b** as a yellow oil (1.2 g, 5%): ¹H NMR (300 MHz) δ 0.09 (6H, s), 0.94 (s, 9H), 3.70 (s, 3H), 3.77 (s, 3H), 3.92 (s, 3H), 6.34 (d, 1H, $J = 1.8$ Hz), 6.42 (d, 1H, $J = 12$ Hz), 6.43 (d, 1H, $J = 1.8$ Hz), 6.54 (d, 1H, $J = 12$ Hz), 6.92 (d, 1H, $J = 8.7$ Hz), 7.41 (dd, 1H, $J = 2.1$ Hz, $J = 8.9$ Hz), 7.74 (d, 1H, $J = 2.1$ Hz); HRMS calcd for C₂₃H₃₂NO₆Si 446.19989 [M + H]⁺, found 446.20599.

3,3'-Dinitro-4,4',5-trimethoxy-Z-stilbene (20g). The preceding Wittig reaction (see **20a**) was carried out with 3-nitro-4,5-dimethoxybenzaldehyde **18b**²⁰ (0.5 g, 2.37 mmol), phosphonium salt **19b**¹⁹ (1.2 g, 2.36 mmol), sodium hydride (0.3 g, 7.5 mmol, 60% in mineral oil), and toluene (200 mL). Purification by flash chromatography on silica gel using hexane–ethyl acetate (1:1) as eluent afforded dinitrostilbene **20g** as an off-white powder (0.47 g, 55%): mp 114–115 °C; ¹H NMR (300 MHz) δ 3.72 (s, 3H), 3.95 (s, 3H), 3.98 (s, 3H), 6.57 (d, 2H, $J = 3.0$ Hz), 6.95 (d, 1H, $J = 1.5$ Hz), 6.98 (d, 1H, $J = 9.0$ Hz), 7.20 (d, 1H, $J = 1.8$ Hz), 7.40 (dd, 1H, $J = 2.0$ Hz, $J = 6.2$ Hz), 7.75 (d, 1H, $J = 2.1$ Hz); HRMS calcd for C₁₇H₁₇N₂O₇ 361.10365 [M + H]⁺, found 361.10358.

General Procedure for Cleavage of the Silyl Ether Protecting Group. 3-Fluoro-4,4',5-trimethoxy-3'-hydroxy-Z-stilbene (11a, Fluorcombstatin). A solution prepared from *Z*-isomer **8a** (2.4 g, 4.4 mmol), tetrahydrofuran (50 mL), and 1 M tetrabutylammonium fluoride (4.5 mL, 4.5 mmol) was stirred for 3 h. The reaction was terminated by the addition of H₂O (50 mL), the mixture was extracted with ethyl acetate, and solvents were removed in vacuo. Separation by flash

Table 4. Antimicrobial Activities of Fluorcombstatin (**11a**) and Related Compounds^a

microorganism	range of minimum inhibitory concentration ($\mu\text{g/mL}$)					
	11a	11b	12a	13a	13b	16a
<i>Cryptococcus neoformans</i> ATCC 90112	64	64	64	*	*	*
<i>Candida albicans</i> ATCC 90028	*	*	*	*	*	*
<i>Staphylococcus aureus</i> ATCC 29213	*	32–64	*	*	*	*
<i>Streptococcus pneumoniae</i> ATCC 6303	64	64	32–64	*	*	*
<i>Enterococcus faecalis</i> ATCC 29212	*	*	*	*	*	*
<i>Micrococcus luteus</i> Presque Isle 456	32–64	16–32	32	32–64	*	*
<i>Escherichia coli</i> ATCC 25922	*	*	*	*	*	*
<i>Enterobacter cloacae</i> ATCC 13047	*	*	*	*	*	*
<i>Stenotrophomonas maltophilia</i> ATCC 13637	*	*	*	*	*	*
<i>Neisseria gonorrhoeae</i> ATCC 49226	32	8–16	16	32–64	*	16

^a * = no inhibition at 64 $\mu\text{g/mL}$.

chromatography with 1:4 ethyl acetate–hexane as eluent provided *Z*-stilbene **11a** (1.12 g, 83%) as a colorless solid, which was recrystallized from ethyl acetate–hexane: mp 93–94 °C; ¹H NMR (300 MHz, CDCl₃) δ 3.67 (s, 3H), 3.87 (s, 3H), 3.90 (d, 1H, $J_{\text{HF}} = 0.9$ Hz), 5.30 (bs, 1H), 6.35 (d, 1H, $J = 12$ Hz), 6.48 (d, 1H, $J = 12$ Hz), 6.61–6.66 (m, 2H), 6.72 (d, 1H, $J = 8.4$ Hz), 6.75–6.84 (m, 2H), 6.86 (d, 1H, $J = 1.5$ Hz); ¹³C NMR (75 MHz, CDCl₃) δ 55.9, 56.0, 61.4 (d, $J_{\text{CF}} = 3.5$ Hz), 108.2, 109.4, 109.6, 110.33, 114.8, 120.9, 127.7, 127.7, 130.0, 130.1, 132.4, 132.5, 135.8, 135.9, 145.1, 145.8, 152.8, 152.9, 154.2, 156.6; ¹⁹F NMR (CDCl₃) δ –11.32 (d, $J = 12.8$ Hz, 1F); HRMS calcd for C₁₇H₁₈FO₄ 305.1189 [M + H]⁺, found 305.1187; *anal.* calcd for C₁₇H₁₇FO₄ C, H.

3-Fluoro-4,4',5-trimethoxy-3'-hydroxy-*E*-stilbene (11b). Cleavage of silyl ester **8b** (150 mg, 0.27 mmol) was performed as described for the synthesis of **11a**. Separation by flash chromatography on silica using ethyl acetate–hexane (3:7) gave the title compound (75 mg, 88%). Recrystallization from hexane gave a colorless solid: mp 86–87 °C; ¹H NMR (300 MHz, CDCl₃) δ 3.91 (s, 3H), 3.92 (s, 3H), 3.93 (d, $J_{\text{HF}} = 0.9$ Hz), 5.75 (bs, 1H), 6.77–6.98 (m, 6H), 6.86 (d, 1H, $J = 1.8$ Hz); ¹³C NMR (75 MHz, CDCl₃) δ 55.9, 56.2, 61.4, 100.6, 105.7, 106.5, 106.8, 107.5, 110.6, 111.8, 119.3, 125.8, 127.6, 128.6, 129.5, 130.6, 133.1, 133.2, 134.7, 136.4, 145.8, 146.6, 153.6, 156.0 (d, $J_{\text{CF}} = 242$ Hz, *ipso* C); *anal.* calcd for C₁₇H₁₇FO₄ C, 67.10%; H, 5.63%, found C, 66.66%; H, 6.51%.

3-Chloro-4,4',5-trimethoxy-3'-hydroxy-*Z*-stilbene (12a). Deprotection of silyl ester **9a** (1.5 g, 2.7 mmol) was conducted as summarized for the synthesis of **11a**. Separation by flash chromatography on silica using ethyl acetate–hexane (3:7) gave the title compound (754 mg, 89%). Recrystallization from hexane gave a white solid: mp 105–106 °C; ¹H NMR (500 MHz, CDCl₃) δ 3.65 (s, 3H), 3.86 (s, 3H), 3.88 (s, 3H), 5.52 (s, 1H), 6.36 (d, 1H, $J = 12$ Hz), 6.50 (d, 1H, $J = 12$ Hz), 6.72–6.76 (m, 3H), 6.88 (dd, 2H, $J = 1.5$ Hz, $J = 6$ Hz); ¹³C NMR (75 MHz, CDCl₃) δ 55.9, 55.9, 60.8, 110.4, 111.4, 114.9, 121.0, 122.5, 127.6, 127.9, 130.1, 130.4, 133.7, 144.4, 145.3, 145.9, 153.2; *anal.* calcd for C₁₇H₁₇ClO₄ C, H.

3-Chloro-4,4',5-trimethoxy-3'-hydroxy-*E*-stilbene (12b). Removal of the silyl group from **9b** (5.6 g, 6.0 mmol) was as described for the synthesis of **11a**. Purification by flash chromatography on silica using ethyl acetate–hexane (3:7) gave the title compound (1.62 g, 79%). Recrystallization from hexane led to a colorless solid: mp 138–140 °C; ¹H NMR (300 MHz, CDCl₃) δ 3.87 (s, 3H), 3.88 (s, 3H), 3.90 (s, 3H), 5.69 (bs, 1H), 6.79 (d, 1H, $J = 15.9$ Hz), 6.81 (d, 1H, $J = 8.4$ Hz), 6.84–6.96 (m, 3H), 7.10 (dd, $J = 1.8$ Hz, $J = 8.4$ Hz); ¹³C NMR (75 MHz, CDCl₃) δ 55.9, 56.1, 60.7, 108.7, 110.6, 111.8, 119.4, 119.8, 125.5, 128.4, 128.8, 130.6, 134.2, 144.6, 145.8, 146.6, 153.8; HRMS calcd for C₁₇H₁₇ClO₄ ³⁵Cl 321.0894 [M + H]⁺, found 321.0893; *anal.* calcd for C₁₇H₁₇ClO₄ C, H.

3-Bromo-4,4',5-trimethoxy-3'-hydroxy-*Z*-stilbene (13a). The silyl ester cleavage reaction for **10a** (4 g, 6.6 mmol) was completed as described for the synthesis of phenol **11a**. Isolation by flash column chromatography on silica gel using ethyl acetate–hexane (1:4) gave **13a** (2.22 g, 92%). Recrystallization from hexane afforded a colorless solid: mp 108–109 °C; IR 3539, 3411, 3011, 2939, 2839, 1554, 1510, 1273, 1047,

908, 732 cm⁻¹; ¹H NMR (300 MHz, CDCl₃) δ 3.63 (s, 3H) 3.84 (s, 3H), 3.86 (s, 3H), 6.34 (d, 1H, $J = 12$ Hz), 6.49 (d, 1H, $J = 12$ Hz), 6.73 (d, 1H, $J = 8.4$ Hz), 6.77 (d, 1H, $J = 8.7$, 1.8 Hz), 6.79 (d, 1H, $J = 1.8$ Hz), 6.86 (d, 1H, $J = 1.5$ Hz), 7.04 (d, 1H, $J = 1.5$ Hz); ¹³C NMR (75 MHz, CDCl₃) δ 55.8, 55.9, 60.6, 110.4, 112.1, 115.0, 117.2, 121.0, 125.3, 127.3, 130.1, 130.4, 134.4, 145.3, 146.0, 153.0; HRMS calcd for C₁₇H₁₇O₄⁸¹Br 366.0290 [M + H]⁺, found 366.0287; *anal.* calcd for C₁₇H₁₇BrO₄ C, H.

3-Bromo-4,4',5-trimethoxy-3'-hydroxy-*E*-stilbene (13b). By the same procedure used to obtain phenol **13a**, silyl ester **10b** was converted to *E* phenol **13b** and isolated by flash column chromatography on silica gel with ethyl acetate–hexane (3:7) as eluent to provide the title compound (0.14 g, 81%). Recrystallization from hexane gave a colorless solid: mp 152–154 °C; ¹H NMR (300 MHz, CDCl₃) δ 3.86 (s, 3H), 3.89 (s, 3H), 3.90 (s, 3H), 6.80 (d, 1H, $J = 15.9$ Hz), 6.82 (d, 1H, $J = 8.4$ Hz), 6.94–6.97 (m, 1H), 6.88 (s, 1H), 7.11 (d, 1H, $J = 1.8$ Hz), 7.25 (d, 1H, $J = 1.5$ Hz), 7.28 (d, 1H, $J = 15.9$ Hz); ¹³C NMR (75 MHz, CDCl₃) δ 56.0, 56.1, 60.6, 109.3, 110.6, 11.7, 117.8, 119.3, 122.6, 125.3, 128.8, 130.5, 134.8, 145.6, 145.7, 146.5, 153.5; *anal.* calcd for C₁₇H₁₇BrO₄ C, H.

3-Hydroxy-4,4',5-trimethoxy-3'-nitro-*Z*-stilbene (20c). Cleavage of the silyl ester **20a** (0.15 g, 70.34 μmol) was performed as noted for the synthesis of phenol **11a** to provide phenol **20c** (0.11 g, 99%) as a yellow oil: ¹H NMR (300 MHz, CDCl₃) δ 3.69 (s, 3H), 3.90 (s, 3H), 3.92 (s, 3H), 5.70 (s, 1H), 6.35 (s, 1H), 6.41 (d, 1H, $J = 12.5$ Hz), 6.49 (d, 1H, $J = 1.5$ Hz), 6.53 (d, 1H, $J = 12.5$ Hz), 6.92 (d, 1H, $J = 8.5$ Hz), 7.40 (dd, 1H, $J = 2.1$ Hz, $J = 9$ Hz) and 7.72 (d, 1H, $J = 2.1$ Hz); HRMS calcd for C₁₇H₁₈NO₆ 332.1134 [M + H]⁺, found 332.1108; *anal.* calcd for C₁₇H₁₇NO₆ C, H, N.

3-Hydroxy-4,4',5-trimethoxy-3'-nitro-*E*-stilbene (20d). The preceding cleavage reaction was repeated using **20b** (175 mg, 0.39 mmol), and following separation by flash column chromatography on silica gel, phenol **20d** (76 mg, 66%) was obtained as a yellow oil: mp 123–124 °C; FABMS calcd for C₁₇H₁₇NO₆ 331.1056, found *m/z* 331 [M]⁺.

3-Hydroxy-4,4',5-trimethoxy-3'-amino-*Z*-stilbene (20e) and Hydrochloride (20f). Platinum-on-carbon (5%, 0.5 g) was added to a solution of *Z*-stilbene **20c** (1.2 g, 3.62 mmol) and ammonium formate (1.0 g, 15.85 mmol) in MeOH (5 mL). The mixture was heated under reflux for 30 min and filtered, and the residue was fractionated on a column of silica gel in 7:3 hexane–ethyl acetate to yield amine **20e** (0.94 g, 86%) as an amorphous yellow solid: ¹H NMR (400 MHz, CDCl₃) δ 3.59 (s, 3H), 3.75 (s, 3H), 3.81 (s, 3H), 6.25 (d, 1H, $J = 12$ Hz), 6.35 (d, 1H, $J = 12$ Hz), 6.38 (d, 1H, $J = 2$ Hz), 6.47 (d, 1H, $J = 1.6$ Hz), 6.60 (s, 1H), 6.61 (s, 1H), 6.62 (s, 1H); ¹³C NMR (75 MHz w/APT) 55.5n, 55.6n, 61.0n, 104.9n, 108.8n, 110.1n, 115.4n, 119.5n, 128.2n, 130.0p, 130.0n, 133.5p, 134.5p, 135.7p, 146.6p, 148.9p, 151.8p; FABMS calcd for C₁₇H₁₉NO₄ 301.13, found *m/z* 301 [M]⁺. A solution of amine **20e** (1.0 g, 3.32 mmol) in ether (5 mL) was treated with ethereal hydrogen chloride (1 M, 5 mL), and the product was collected as a pale yellow solid (**20f**, 1.14 g, 99%): mp 153–156 °C; ¹H NMR (500 MHz, D₂O) δ 3.48 (s, 3H), 3.62 (s, 3H), 3.76 (s, 3H), 6.29 (s, 1H), 6.32 (s, 1H), 6.36 (d, 1H, $J = 12$ Hz), 6.42 (d, 1H, $J = 12$ Hz), 6.89 (d, 1H,

$J = 8.5$ Hz), 7.09 (s, 1H), 7.13 (s, 1H); ^{13}C NMR (75 MHz, D_2O , w/APT) 55.9p, 56.3p, 61.0p, 105.6p, 110.0p, 112.4p, 118.9n, 124.0p, 128.7p, 129.9p, 130.2n, 131.0p, 133.6n, 135.8n, 149.0n, 151.7n, 152.7n; HRMS calcd for $\text{C}_{17}\text{H}_{20}\text{NO}_4$ 302.1392 [$\text{M} + \text{H}$] $^+$, found 302.1381.

3,3'-Diamino-4,4',5-trimethoxy-Z-stilbene (20h). To dinitrostilbene **20g** (0.11 g, 0.31 mmol) in acetic acid (25 mL) was added zinc powder (4 g, 61.2 mmol). After 1 h the mixture was filtered through Celite and the solvent was removed in vacuo to yield diamine **20h** as a yellow oil (72 mg, 75%): ^1H NMR (300 MHz) δ 3.66 (s, 3H), 3.73 (br s, 4H), 3.81 (s, 3H), 3.83 (s, 3H), 6.32 (s, 1H), 6.35 (d, 1H, $J = 2.1$ Hz), 6.35 (dd, 2H, $J = 12.0$ Hz, $J = 13.2$ Hz), 6.67 (s, 1H), 6.68 (s, 1H), 6.71 (s, 1H); HRMS calcd for $\text{C}_{17}\text{H}_{21}\text{N}_2\text{O}_3$ 301.1552 [$\text{M} + \text{H}$] $^+$, found 301.1639; *anal.* calcd for $\text{C}_{17}\text{H}_{20}\text{N}_2\text{O}_3$ C, H.

Dibenzyl 3-fluoro-4,4',5-trimethoxy-Z-stilbene 3'-O-phosphate (14). A solution of phenol **11a** (1.1 g, 3.6 mmol), acetonitrile (20 mL), and 3.5 mL (36 mmol) of CCl_4 was cooled to -10°C and stirred for 10 min. Then diisopropyl ethylamine (1.3 mL, 7.4 mmol) and DMAP (44 mg, 0.36 mmol) were added. After 1 min, dibenzyl phosphite (1.2 mL, 5.4 mmol) was added (over 5 min), and the mixture stirred for an additional 3 h at -10°C . The reaction was terminated by the addition of 0.5 M KH_2PO_4 , the mixture was extracted with ethyl acetate, solvents were removed in vacuo, and the product was isolated by flash chromatography (1:1 elution with ethyl acetate-hexane) to yield phosphate **14** (1.5 g, 74%): bp dec 280°C (0.01 mmHg); ^1H NMR (300 MHz, CDCl_3) δ 3.65 (s, 3H), 3.77 (s, 3H), 3.87 (d, 3H, $J_{\text{HF}} = 1.2$ Hz), 5.12 (s, 2H), 5.14 (s, 2H), 6.38 (d, 1H, $J = 12$ Hz), 6.43 (d, 1H, $J = 12$ Hz), 6.57 (s, 1H), 6.62 (dd, 1H, $J = 1.5$ Hz, $J = 11.5$ Hz), 6.78 (d, 1H, $J = 8.5$ Hz), 7.03 (d, 1H, $J = 8.5$ Hz), 7.12 (s, 1H), 7.14–7.32 (m, 10H); ^{13}C NMR (100 MHz, CDCl_3) δ 55.8, 61.4 (d, $J_{\text{CF}} = 3$ Hz), 69.7, 69.7, 108.1, 108.2, 109.5 (d, $J_{\text{CF}} = 20.45$ Hz, *ortho*), 112.3, 126.4, 126.4, 127.8, 128.4, 128.5, 129.3, 129.6, 129.6, 132.2 (d, $J_{\text{CF}} = 9.1$ Hz, *meta* C), 135.6, 135.7, 139.4, 139.5, 149.9, 149.9, 153.1, 153.1, 155.6 (d, $J_{\text{CF}} = 243$ Hz, *ipso* C); ^{31}P NMR (162 MHz CDCl_3) δ -7.84; HRMS calcd for $\text{C}_{31}\text{H}_{30}\text{FO}_7\text{P}$ 565.1791 [$\text{M} + \text{H}$] $^+$, found 565.1812; *anal.* calcd for $\text{C}_{31}\text{H}_{30}\text{FO}_7\text{P}$ C, H.

Dibenzyl 3-bromo-4,4',5-trimethoxy-Z-stilbene 3'-O-phosphate (15). Phosphorylation of **13a** (1 g, 2.7 mmol) was performed as described for the synthesis of phosphate **14**. Separation by flash column chromatography on silica using ethyl acetate-hexane (1:1) as eluent gave phosphate **15** (1.6 g, 94%) as an oil: bp dec 271°C (0.01 mmHg); ^1H NMR (300 MHz, CDCl_3) δ 3.59 (s, 3H), 3.76 (s, 3H), 3.79 (s, 3H), 5.11 (s, 2H), 5.13 (s, 2H), 6.37 (d, 1H, $J = 12$ Hz), 6.43 (d, 1H, $J = 12$ Hz), 6.72 (d, 1H, $J = 1.5$ Hz), 6.78 (d, 1H, $J = 8.4$ Hz), 7.01–7.04 (m, 1H), 7.03 (d, 1H, $J = 2.4$ Hz), 7.10 (d, 1H, $J = 1.8$ Hz), 7.28–7.35 (m, 10H); ^{13}C NMR (100 MHz, CDCl_3) δ 55.8, 55.9, 60.5, 65.1, 69.7, 69.7, 111.8, 112.2, 117.2, 122.0, 122.0, 125.0, 126.3, 126.7, 127.3, 127.7, 127.8, 127.9, 128.3, 128.4, 129.3, 129.5, 129.5, 133.9, 135.4, 135.5, 139.3, 139.4, 145.3, 149.8, 149.8, 153.0; ^{31}P NMR (162 MHz CDCl_3) δ -7.84; HRMS calcd for $\text{C}_{31}\text{H}_{31}\text{BrO}_7\text{P}$ 625.0991 [$\text{M} + \text{H}$] $^+$, found 625.0928, ^{81}Br 627.0970 [$\text{M} + \text{H}$] $^+$, found 627.09704; *anal.* calcd for $\text{C}_{31}\text{H}_{30}\text{BrO}_7\text{P}$ C, H.

General Procedure for Synthesis of the Phosphate Cation Derivatives. Method A. Each of the metal cation containing salts was obtained by the procedure outlined directly below for preparing sodium salt **16a**. The metal counterions were introduced by treatment of the phosphoric acid with either the corresponding hydroxide (potassium, lithium) or acetate (magnesium).

Sodium 3-fluoro-4,4',5-trimethoxy-Z-stilbene 3'-O-phosphate (16a). To a cooled solution of dibenzyl phosphate **14** (1.02 g, 1.8 mmol) in dry CH_2Cl_2 (40 mL) was added trimethylsilylbromide (530 μL , 3.9 mmol). The reaction mixture was stirred at 0°C for 2 h under argon, then terminated with 10% sodium thiosulfate solution (8 mL). The organic layer was separated and extracted with CH_2Cl_2 (3 \times 40 mL). The combined organic layers were dried, filtered, and concentrated. The free phosphoric acid was dissolved in MeOH (5 mL), and NaOMe (195 mg, 3.6 mmol) was added to the solution. After the reaction mixture was stirred for 30 min, the precipitate

was collected and washed with ether to provide sodium salt **16a** (0.61 g, 76%): colorless solid; mp $200\text{--}202^\circ\text{C}$; ^1H NMR (300 MHz, D_2O) δ 3.52 (s, 3H), 3.67 (s, 3H), 3.68 (s, 3H), 6.52 (d, 1H, $J = 12$ Hz), 6.71 (d, 1H, $J = 12$ Hz), 6.72 (s, 1H), 6.78 (s, 1H), 6.79 (s, 1H), 7.03 (s, 1H), 7.16 (s, 1H).

Lithium 3-fluoro-4,4',5-trimethoxy-Z-stilbene 3'-O-phosphate (16b): colorless solid; mp $255\text{--}274^\circ\text{C}$; ^1H NMR (300 MHz, D_2O) δ 3.55 (s, 3H), 3.68 (s, 3H), 3.72 (s, 3H), 6.36 (d, 1H, $J = 12$ Hz), 6.51 (d, 1H, $J = 12$ Hz), 6.62–6.65 (m, 2H), 6.69–6.76 (m, 2H), 7.22 (s, 1H).

Potassium 3-fluoro-4,4',5-trimethoxy-Z-stilbene 3'-O-phosphate (16c): colorless solid; mp $192\text{--}210^\circ\text{C}$; ^1H NMR (300 MHz, D_2O) δ 3.56 (s, 3H), 3.69 (s, 3H), 3.74 (s, 3H), 6.37 (d, 1H, $J = 12$ Hz), 6.51 (d, 1H, $J = 12$ Hz), 6.62–6.78 (m, 4H), 7.24 (s, 1H).

Sodium 3-bromo-4,4',5-trimethoxy-Z-stilbene 3'-O-phosphate (17a). To a solution of dibenzyl phosphate **15** (0.28 g, 0.45 mmol) in dry CH_2Cl_2 (10 mL) was added trimethylsilylbromide (125 μL , 0.95 mmol). The reaction mixture was stirred for 30 min under argon, and the reaction was terminated by the addition of MeOH (20 mL). Following removal of solvents (in vacuo), the phosphoric acid was dissolved in EtOH (10 mL), and NaOMe (49 mg, 0.9 mmol) was added to the solution. After the reaction mixture was stirred for 30 min, the precipitate was collected and washed with ether to provide sodium salt **17a** (0.17 g) as a colorless solid: mp $196\text{--}197^\circ\text{C}$; ^1H NMR (300 MHz, D_2O) δ 3.53 (s, 3H), 3.68 (s, 3H), 3.70 (s, 3H), 6.37 (d, 1H, $J = 12$ Hz), 6.52 (d, 1H, $J = 12$ Hz), 6.75 (s, 1H), 6.77 (s, 1H), 6.79 (s, 1H), 7.01 (s, 1H), 7.15 (s, 1H).

Lithium 3-bromo-4,4',5-trimethoxy-Z-stilbene 3'-O-phosphate (17b): colorless solid; mp $265\text{--}268^\circ\text{C}$ (dec); ^1H NMR (300 MHz, D_2O) δ 3.53 (s, 3H), 3.66 (s, 3H), 3.69 (s, 3H), 6.35 (d, 1H, $J = 12$ Hz), 6.52 (d, 1H, $J = 12$ Hz), 6.70 (s, 2H), 6.81 (d, 1H, $J = 1.5$ Hz), 7.01 (d, 1H, $J = 1.5$ Hz), 7.23 (s, 1H).

Potassium 3-bromo-4,4',5-trimethoxy-Z-stilbene 3'-O-phosphate (17c): colorless solid; mp $230\text{--}233^\circ\text{C}$ (dec); ^1H NMR (300 MHz, D_2O) δ 3.53 (s, 3H), 3.66 (s, 3H), 3.69 (s, 3H), 6.35 (d, 1H, $J = 12$ Hz), 6.52 (d, 1H, $J = 12$ Hz), 6.70 (s, 2H), 6.81 (d, 1H, $J = 1.5$ Hz), 7.01 (d, 1H, $J = 1.5$ Hz), 7.23 (s, 1H).

Cesium 3-bromo-4,4',5-trimethoxy-phenyl-Z-stilbene 3'-O-phosphate (17d): colorless solid; mp $233\text{--}235^\circ\text{C}$; ^1H NMR (300 MHz, DMSO) δ 3.51 (s, 3H), 3.62 (s, 3H), 3.65 (s, 3H), 6.38 (d, 1H, $J = 12$ Hz), 6.50 (d, 1H, $J = 12$ Hz), 6.71 (s, 1H), 6.83 (d, 1H, $J = 1.5$ Hz), 7.03 (d, 2H, $J = 1.5$ Hz), 7.23 (s, 1H).

Rubidium 3-bromo-4,4',5-trimethoxy-Z-stilbene 3'-O-phosphate (17e): colorless solid; mp $204\text{--}206^\circ\text{C}$; ^1H NMR (300 MHz, DMSO) δ 3.50 (s, 3H), 3.64 (s, 3H), 3.66 (s, 3H), 6.35 (d, 1H, $J = 12$ Hz), 6.52 (d, 1H, $J = 12$ Hz), 6.68 (s, 2H), 6.80 (d, 2H, $J = 1.5$ Hz), 7.00 (d, 2H, $J = 1.5$ Hz), 7.25 (s, 1H).

Calcium 3-bromo-4,4',5-trimethoxy-Z-stilbene 3'-O-phosphate (17f): colorless solid; mp $245\text{--}248^\circ\text{C}$ (dec); ^1H NMR (300 MHz, DMSO) δ 3.53 (s, 3H), 3.69 (s, 3H), 3.70 (s, 3H), 6.33 (d, 1H, $J = 12$ Hz), 6.50 (d, 1H, $J = 12$ Hz), 6.71 (s, 2H), 6.81 (d, 2H, $J = 1.5$ Hz), 7.99 (d, 2H, $J = 1.5$ Hz), 7.23 (s, 1H).

Magnesium 3-bromo-4,4',5-trimethoxy-Z-stilbene 3'-O-phosphate (17g): colorless solid; mp $280\text{--}285^\circ\text{C}$ (dec); ^1H NMR (300 MHz, DMSO) δ 3.50 (s, 3H), 3.60 (s, 3H), 3.65 (s, 3H), 6.33 (d, 1H, $J = 12$ Hz), 6.50 (d, 1H, $J = 12$ Hz), 6.68 (s, 2H), 6.79 (d, 2H, $J = 1.5$ Hz), 7.00 (d, 2H, $J = 1.5$ Hz), 7.21 (s, 1H).

Method B. The potassium salt **16c** (~ 30 mg) was dissolved in deionized H_2O (1 mL) and applied to a Dowex-50w (HCR-W2) resin column (amine or amino acid) and eluted with water. The eluent was concentrated by freeze-drying to give the required compound.

Morpholine 3-fluoro-4,4',5-trimethoxy-Z-stilbene 3'-O-phosphate (16d): colorless oil; ^1H NMR (300 MHz, D_2O) δ 3.10–3.14 (m, 8H), 3.54 (s, 3H), 3.67 (s, 3H), 3.71 (s, 3H), 3.76–3.81 (m, 8H), 6.35 (d, 1H, $J = 12$ Hz), 6.49 (d, 1H, $J = 12$ Hz), 6.59–6.36 (m, 2H), 6.76–6.76 (m, 2H), 7.18 (s, 1H).

Piperidine 3-fluoro-4,4',5-trimethoxy-Z-stilbene 3'-O-phosphate (16e): waxy colorless solid; mp $55\text{--}57^\circ\text{C}$; ^1H NMR (300 MHz, D_2O) δ 1.47–1.59 (m, 12H), 2.94–3.03 (m,

8H), 3.51 (s, 3H), 3.64 (s, 3H), 3.67 (s, 3H), 6.30 (d, 1H, $J = 12$ Hz), 6.48 (d, 1H, $J = 12$ Hz), 6.56–6.72 (m, 4H), 7.20 (s, 1H).

Glycine-Ome 3-fluoro-4,4',5-trimethoxy-Z-stilbene 3'-O-phosphate (16f): colorless waxy solid; mp 88–92 °C; ^1H NMR (300 MHz, D_2O) δ 3.53 (s, 2H), 3.68 (s, 2H), 3.71 (s, 3H), 3.76 (s, 3H), 6.35 (d, 1H, $J = 12$ Hz), 6.49 (d, 1H, $J = 12$ Hz), 6.58–6.62 (m, 2H), 6.72–6.81 (m, 2H), 7.13 (s, 1H).

Tryptophan-Ome 3-fluoro-4,4',5-trimethoxy-Z-stilbene 3'-O-phosphate (16g): colorless solid; mp 75–80 °C; ^1H NMR (300 MHz, D_2O) δ 3.24 (d, 2H, $J = 6$ Hz), 3.53 (s, 3H), 3.61 (s, 3H), 3.67 (s, 3H), 3.72 (s, 3H), 4.11 (t, 1H, $J = 6$ Hz), 6.35 (d, 1H, $J = 12$ Hz), 6.60–6.64 (m, 2H), 7.04 (t, 1H, $J = 7.5$ Hz), 7.09–7.14 (m, 2H), 7.20 (s, 1H), 7.38 (d, 1H, $J = 7.8$ Hz), 7.46 (d, $J = 7.5$ Hz).

Tris' 3-fluoro-4,4',5-trimethoxy-Z-stilbene 3'-O-phosphate (16h): colorless solid; mp 88–93 °C; ^1H NMR (300 MHz, DMSO) δ 3.34 (s, 12H), 3.62 (s, 3H), 3.70 (s, 3H), 3.75 (s, 3H), 6.36 (d, 1H, $J = 12$ Hz), 6.49 (d, 1H, $J = 12$ Hz), 6.66–6.71 (m, 1H), 6.75–6.77 (m, 2H), 6.81 (d, 1H, $J = 8.4$ Hz), 7.42 (s, 1H).

Cancer Cell Line Procedures. Inhibition of human cancer cell growth was assessed using the National Cancer Institute's standard sulforhodamine B assay as previously described.²¹ After 48 h, the plates were fixed with trichloroacetic acid, stained with sulforhodamine B, and read with an automated microplate reader. A growth inhibition of 50% (GI_{50} , or the drug concentration causing a 50% reduction in the net protein increase) was calculated from optical density data with Immunosoft software. Inhibition of the mouse leukemia P388 cells was assessed in a 10% horse serum/Fisher medium solution for 24 h, followed by a 48 h incubation with serial dilutions of the compounds. Cell growth inhibition (ED_{50}) was then calculated using a Z1 Beckman/Coulter particle counter.

Tubulin Evaluations. Tubulin polymerization was evaluated by turbidimetry at 350 nm using Beckman DU7400/7500 spectrophotometers as described in detail elsewhere.²⁰ Varying concentrations of drug were preincubated with 10 μM (1.0 mg/mL) purified tubulin,²³ samples were chilled on ice, GTP (0.4 mM) was added, and polymerization was followed at 30 °C. The parameter measured was extent of the reaction after 20 min. Colchicine binding was measured as described in detail previously.²⁴ Reaction mixtures contained 1.0 μM tubulin, 5.0 μM [^3H]colchicine (from Dupont), and inhibitor at 1.0 μM . Incubation was for 10 min at 37 °C.

Antiangiogenesis Evaluation. HUVEC Procedures. Method A. Umbilical cords were obtained from the Maternity Unit at Bradford Royal Infirmary following ethical approval and consent from mothers. Isolated HUVECs were grown in medium M199 (Sigma) supplemented with 20% human serum. Authentication of cells was by staining for expression of the endothelial cell marker CD31. Cover slips were initially coated with 2% gelatin (Sigma) for 30 min and washed with Hanks medium (Sigma) before being placed individually in 24-well plates. Growth medium M199 (1 mL) was added, followed by approximately 3×10^4 HUVECs to give a final volume of 1.5 mL in each well. The cells were incubated at 37 °C for 24 h and checked microscopically before being treated with test compounds.

Test compounds were dissolved in DMSO and added to medium to give a final concentration of 1 μM , 10 μM , or 100 μM in each well. Duplicate plates were prepared for each compound, and at time points of 30 min, 1, 2, and 4 h, the appropriate set of cover slips was removed and fixed in ice-cold methanol for at least 1 h. Untreated controls were treated identically. The cover slips were then washed in PBS for 10 min before being incubated with 100 μL monoclonal anti-human α -tubulin (mouse IgG1 isotype, Sigma) diluted 1:500 with PBS for 30 min. Following three 5 min washes with PBS, 100 μL of the secondary antibody TRITC (tetramethylrhodamine isothiocyanate)-conjugated rabbit anti-mouse immunoglobulin (DAKO) was added to each cover slip at a concentration of 1:50 in PBS. This and all subsequent staining procedures were carried out in the dark. After a 30 min incubation period, the cover slips were washed again in PBS (three 5 min washes) before being stained for DNA using

Hoechst 33342 (Sigma, stock solution diluted with PBS to give a final concentration of 1 $\mu\text{g}/\text{mL}$). Following the 30 min incubation, the cover slips were again washed in PBS for 10 min and finally mounted using fluorescent mounting medium (DAKO).

Immunofluorescence microscopy using a confocal microscope was then carried out to assess any disruption of the microtubules in the cells. The cells were scored for tubulin disruption (Table 3) and the results tabulated. Images to support the scoring were also obtained.

Method B. In vitro Matrigel antiangiogenesis assays were implemented according to the Developmental Therapeutics Program NCI/NIH protocols.²² Matrigel, a basement membrane matrix, was purchased from BD Biosciences. Growth inhibition and cord formation assays were conducted using HUVECs purchased from GlycoTech. HUVEC cells were grown in EGM-2 medium (Cambrex).

Cord Formation Assay. An aliquot of Matrigel (60 μL) was placed in each well of an ice-cold 96-well plate. The plates were incubated 15 min at RT, followed by 30 min at 37 °C, to permit the Matrigel to polymerize. Meanwhile, HUVECs were harvested and diluted to a concentration of 2×10^5 cells/mL, and 100 μL of the cell suspension was added to each well. A second solution of 100 μL containing the compounds to be tested was added next. After 24 h incubation, images were taken for each concentration using an inverted Nikon Diaphot microscope and D100 digital camera. Drug effect was assessed in comparison to untreated controls by measuring the length of cords formed and number of junctions.

The standard sulforhodamine B assay (see Cancer Cell Line Procedures above) was used to evaluate results using HUVECs. The ED_{50} (drug concentration causing 50% inhibition) was calculated from the plotted data.

Broth Microdilution Susceptibility Testing of Bacteria. The antibacterial activity of a subset of the halocombstatins was assessed by the NCCLS broth microdilution assay (BMA).¹⁷ The halocombstatins were reconstituted in a small volume of sterile DMSO and diluted in the appropriate media prior to susceptibility experiments. Isolated colonies from overnight cultures were suspended and diluted as recommended to yield final inocula of approximately 5×10^5 CFU/mL. Tests were performed in sterile 96-well plates containing 2-fold dilutions of the test compounds in gonococcal typing broth (*Neisseria*), Mueller Hinton II (MHII) (cation-adjusted) broth containing 3% lysed horse blood (*Streptococcus*), or MHII broth (all other bacteria). One well was left drug-free (but contained an equivalent volume of DMSO) for a turbidity control. Plates were incubated without agitation at 37 °C with 5% CO_2 (*Neisseria*) or at 35 °C (all other bacteria). MICs were determined at 24 h. The MIC was defined as the lowest drug concentration that inhibited all visible growth of the test organism (optically clear).

Broth Microdilution Susceptibility Testing of Yeasts. The halocombstatins were screened against yeasts by broth microdilution assays (BMAs) according to the NCCLS.¹⁸ Isolated yeast colonies were suspended and diluted as recommended to yield final inocula ranging from 0.5 to 2.5×10^3 CFU/mL. Tests were performed in sterile 96-well plates containing 2-fold dilutions of the test compounds in 0.165 M morpholinepropanesulfonic acid buffered RPMI 1640 medium (pH 7.0). One well was left drug-free (but contained an equivalent volume of DMSO) for a turbidity control. Plates were incubated without agitation at 35 °C. MICs were determined at 48 h for *Candida* and at 72 h for *Cryptococcus*. The MIC was defined as the lowest drug concentration that inhibited all visible growth of the test organism (optically clear).

Acknowledgment. The financial support was provided with our appreciation by Outstanding Investigator Grant CA44344-08-12 and Grant RO1 CA90441-01-05 awarded by the Division of Cancer Treatment and Diagnosis, National Cancer Institute, DHHS; the Arizona Disease Control Research Commission; the Robert S. Dalton Endowment Fund;

Dr. Alec D. Keith; the J. W. Kieckhefer Foundation; the Margaret T. Morris Foundation; the Caitlin Robb Foundation; Gary L. and Diane R. Tooker; Polly J. Trautman; the Eagles Art Ehrmann Cancer Fund; and the Ladies Auxiliary to the Veterans of Foreign Wars. In addition, M.C.B. and S.W.M. acknowledge support from Cancer Research UK, and this study was also assisted in part by NCI, National Institutes of Health Contract NO1-CO-12400. For other helpful assistance, we thank Drs. F. Hogan, J. C. Knight, and J. M. Schmidt, C. Weber, M. J. Dodson, B. Fakoury, F. Craciunescu, and L. Williams.

References and Notes

- (1) For contribution 508, see: Pettit, G. R.; Hogan, F.; Herald, D. L. *J. Org. Chem.* **2004**, *69*, 4019–4022.
- (2) (a) Cooney, M. M.; Radivoyevitch, T.; Dowlati, A.; Overmoyer, B.; Levitan, N.; Robertson, K.; Levine, S. L.; DeCaro, K.; Buchter, C.; Taylor, A.; Stambler, B. S.; Remick, S. *Clin. Cancer Res.* **2004**, *20*, 96–100. (b) Rustin, G. J. S.; Galbraith, S. M.; Anderson, H.; Stratford, M.; Folkes, L. K.; Sena, L.; Gumbrell, L.; Price, P. M. *J. Clin. Oncol.* **2003**, *21*, 2815–2822. (c) Stevenson, J. P.; Rosen, M.; Sun, W.; Gallagher, M.; Haller, D. G.; Vaughn, D.; Giatonio, B.; Zimmer, R.; Petros, W. P.; Stratford, M.; Chaplin, D.; Young, S. L.; Schnall, M.; O'Dwyer, P. J. *J. Clin. Oncol.* **2003**, *21*, 4428–4438.
- (3) (a) Chaplin, D. J. *Pathophysiol. Haemost. Thromb.* **2003**, *33* (Suppl. 1), 9–10. (b) Brooks, A. C.; Kanthou, C.; Cook, I. H.; Tozer, G. M.; Barber, P. R.; Vojnovic, B.; Nash, G. B.; Parkins, C. S. *Anticancer Res.* **2003**, *23*, 3199–3206. (c) Galbraith, S. M.; Maxwell, R. J.; Lodge, M. A.; Tozer, G. M.; Wilson, J.; Taylor, N. J.; Stirling, J. J.; Sena, L.; Padhani, A. R.; Rustin, G. J. S. *J. Clin. Oncol.* **2003**, *21*, 2831–2842. (d) Ahmed, B.; van Euk, L. I.; Bouma-ter Steege, J. C. A.; van der Schaft, W. J.; van Esch, A. M.; Joosten-Achjanie, S. R.; Lambin, P.; Landuyt, W.; Griffioen, A. W. *Int. J. Cancer* **2003**, *105*, 20–25. (e) Griggs, J.; Hesketh, R.; Smith, G. A.; Brindle, K. M.; Metcalfe, J. C.; Thomas, G. A.; Williams, E. *Br. J. Cancer* **2001**, *84*, 832–835.
- (4) (a) Eskens, F. *Br. J. Cancer* **2004**, *90*, 1–7. (b) Hori, K.; Saito, S. *Br. J. Cancer* **2004**, *90*, 549–553. (c) Vogt, T.; Hafner, C.; Bross, K.; Bataille, F.; Jauch, K.-W.; Berand, A.; Landthaler, M.; Andreesen, R.; Reichle, A. *Cancer* **2003**, *98*, 2251–2256. (d) Folkman, J. *Sem. Oncol.* **2001**, *28*, 536–542. (e) Kruger, E. A.; Duray, P. H.; Price, D. K.; Pluda, J. M.; Figg, W. D. *Sem. Oncol.* **2001**, *28*, 570–576. (f) Vacca, A.; Ribatti, D.; Roccaro, A. M.; Frigeri, A.; Dammacco, F. *Sem. Oncol.* **2001**, *28*, 543–550. (g) Rajkumar, S. V.; Kyle, R. A. *Sem. Oncol.* **2001**, *28*, 560–564.
- (5) (a) Wildiers, H.; Ahmed, B.; Guetens, G.; De Boeck, G.; de Bruijn, E. A.; Landuyt, W.; van Oosterom, A. T. *Eur. J. Cancer* **2004**, *40*, 284–290. (b) Newell, D. R.; Searle, K. M.; Westwood, N. B.; Burtles, S. S. *Br. J. Cancer* **2003**, *89*, 437–454. (c) Nabha, S. M.; Mohammad, R. M.; Dandashi, M. H.; Coupaye-Gerard, B.; Aboukameel, A.; Pettit, G. R.; Al-Katib, A. M. *Clin. Cancer Res.* **2002**, *8*, 2735–2741. (d) Griggs, J.; Brindle, K. M.; Metcalfe, J. C.; Hill, S. A.; Smith, G. A.; Beauregard, D. A.; Hesketh, R. *Int. J. Oncol.* **2001**, *821*–825. (e) Nabha, S. M.; Mohammad, R. M.; Wall, N. R.; Dutcher, J. A.; Salkini, B. M.; Pettit, G. R.; Al-Katib, A. M. *Anti-Cancer Drugs* **2001**, *12*, 57–63. (f) Grosios, K.; Loadman, P. M.; Swaine, D. J.; Pettit, G. R.; Bibby, M. C. *Anticancer Res.* **2000**, *20*, 229–234. (g) Nabha, S. M.; Wall, N. R.; Mohammad, R. M.; Pettit, G. R.; Al-Katib, A. M. *Anti-Cancer Drugs* **2000**, *11*, 385–392.
- (6) (a) Pedley, R. B.; Hill, S. A.; Boxer, G. M.; Flynn, A. A.; Boden, R.; Watson, R.; Dearling, J.; Chaplin, D. J.; Begent, R. H. J. *Cancer Res.* **2001**, *61*, 4716–4722. (b) Eikesdal, H. P.; Bjerkvig, R.; Raleigh, J. A.; Mella, O.; Dahl, O. *Radiother. Oncol.* **2001**, *61*, 313–320.
- (7) (a) Pettit, G. R.; Moser, B. R.; Boyd, M. R.; Schmidt, J. M.; Pettit, R. K.; Chapuis, J.-C. *Anti-Cancer Drug Des.* **2001**, *16*, 185–193. (b) Pettit, G. R. Evolutionary Biosynthesis of Anticancer Drugs in Anticancer Agents. In *Frontiers in Cancer Chemotherapy*; Ojima, I., Vite, G. D., Altmann, K.-H., Eds.; American Chemical Society: Washington, DC, 2001; p 16. (c) Pettit, G. R.; Smith, C. R.; Singh, S. B. Recent Advances in the Chemistry of Plant Antineoplastic Constituents. In *Biologically Active Natural Products*; Hostettmann, K., Lea, P. J., Eds.; Clarendon Press: Oxford, England, 1987; p 105.
- (8) Nam, N.-H. *Curr. Med. Chem.* **2003**, *10*, 1697–1722.
- (9) (a) Pettit, G. R.; Lippert, J. W.; Herald, D. L.; Hamel, E.; Pettit, R. K. *J. Nat. Prod.* **2000**, *63*, 969–974. (b) Pettit, G. R.; Lippert, J. W., III. *Anti-Cancer Drug Des.* **2000**, *15*, 203–216. (c) Pettit, G. R.; Minardi, M. D.; Boyd, M. R.; Pettit, R. K. *Anticancer Drug Des.* **2000**, *15*, 397–404.
- (10) Clark, M. T.; Miller, D. D. *J. Org. Chem.* **1986**, *51*, 4072–4073.
- (11) Weinstock, J.; Ladd, D. L.; Wilson, J. W.; Brush, C. K.; Yim, N. C. F.; Gallagher, G. Jr.; McCarthy, M. E.; Silvestri, J.; Sarau, H. M.; Flaim, K. E.; Ackerman, D. M.; Setler, P. E.; Tobia, A. J.; Hahn, R. A. *J. Med. Chem.* **1986**, *29*, 2315–2325.
- (12) Ladd, D. L.; Gaitanopoulos, D. *Synth. Commun.* **1985**, *15*, 61.
- (13) Lin, C. M.; Singh, S. B.; Chu, P. S.; Dempcy, R. O.; Schmidt, J. M.; Pettit, G. R.; Hamel, E. *Mol. Pharmacol.* **1988**, *34*, 200–208.
- (14) Cushman, M.; Nagarathnam, D.; Gopal, D.; He, H.-M.; Lin, C. M.; Hamel, E. *J. Med. Chem.* **1992**, *35*, 2293–2306.
- (15) Bicknell, R.; Lewis, C. E.; Ferrara, N., Eds.; *Tumor Angiogenesis*; Oxford University Press: New York, 1997.
- (16) (a) Grosios, K.; Holwell, S. E.; McGown, A. T.; Pettit, G. R.; Bibby, M. C. *Br. J. Cancer* **1999**, *81*, 1318–1327. (b) Jaffe, E. A.; Nachman, R. L.; Becker, C. G.; Minick, C. R. *J. Clin. Invest.* **1973**, *52*, 2745–2756.
- (17) National Committee for Clinical Laboratory Standards. Methods for Dilution Antimicrobial Susceptibility Tests for Bacteria That Grow Aerobically. Approved Standard M7-A5. Wayne, PA: NCCLS, 2000.
- (18) National Committee for Clinical Laboratory Standards. Reference Method for Broth Dilution Antifungal Susceptibility Testing of Yeasts. Approved Standard M27-A. Wayne, PA: NCCLS, 2002.
- (19) Pinney, K. G.; Mejia, M. P.; Villalobos, V. M.; Rosenquist, B. E.; Pettit, G. R.; Verdier-Pinard, P.; Hamel, E. *Bioorg. Med. Chem.* **2000**, *8*, 2417–2425.
- (20) Hamel, E. *Cell Biochem. Biophys.* **2003**, *38*, 1–21.
- (21) Monks, A.; Scudiero, D.; Skehan, P.; Shoemaker, R.; Paul, K.; Vistica, D.; Hose, C.; Langley, J.; Cronise, P.; Viagro-Wolff, A. *J. Natl. Cancer Inst.* **1991**, *83*, 757–766.
- (22) Developmental Therapeutics Program NCI/NIH, Discovery Services, Angiogenesis Resource Center (http://dtp.nci.nih.gov/aa-resources/aa_index.html).
- (23) Hamel, E.; Lin, C. M. *Biochemistry* **1984**, *23*, 4173–4184.
- (24) Verdier-Pinard, P.; Lai, J. Y.; Yoo, H.-D.; Yu, J.; Marquez, B.; Nagle, D. G.; Nambu, M.; White, J. D.; Falck, J. R.; Gerwick, W. H.; Day, B. W.; Hamel, E. *Mol. Pharmacol.* **1998**, *53*, 62–76. q

NP058038I